Inelastic x-ray scattering from TiC and Ti single crystals

A. T. Macrander

Advanced Photon Source, Argonne National Laboratory, Argonne, Illinois 60439

P. A. Montano

Materials Science Division, Argonne National Laboratory, Argonne, Illinois 60439
and Department of Physics, University of Illinois at Chicago, Chicago, Illinois 60680

D. L. Price

Department of Physics, University of Memphis, Memphis, Tennessee 38152

V. I. Kushnir and R. C. Blasdell

Advanced Photon Source, Argonne National Laboratory, Argonne, Illinois 60439

C. C. Kao

National Synchrotron Light Source, Brookhaven National Laboratory, Upton, New York 11973

B. R. Cooper

Department of Physics, West Virginia University, Morgantown, West Virginia 26506

Inelastic x-ray scattering spectra were measured with incident x rays having an energy near 8 keV for a range of momentum transfers q extending from 0.70 to 2.0 Å^{-1}. We find spectral features corresponding to valence electron excitations, as well as Raman scattering corresponding to excitation from the $3p$ core states to the $3d$ valence states of Ti. The spectral features corresponding to valence electron excitations lie in the regime conventionally interpreted as a bulk plasmon together with intraband and interband transitions. We compare our data for TiC at $q=1.05$ Å^{-1} with calculations for the dynamical dielectric constant $\varepsilon(q,\omega)$ based on local-density theory. The agreement between the data and calculations permits us to interpret certain features in the spectra as arising from band transitions out of the strongly hybridized C $2p$–Ti $3d$ band. The energy loss position of the Raman scattering peak is independent of momentum transfer for both TiC and Ti and lies at 48 eV for Ti. This value is above the highest-lying x-ray ultraviolet absorption resonance for atomic Ti at 43.5 eV. This shift in the data to higher energy transfer is consistent with electron energy loss spectra and photoemission results reported in the literature and indicates that important physical processes are not encompassed within existing theoretical approaches to x-ray Raman scattering. [S0163-1829(96)03425-X]

I. INTRODUCTION

Inelastic x-ray scattering (IXS) spectra are a source of information on the dynamics of electronic excitations.[1] With a bandpass ranging from 0.1 to 1 eV, IXS can be used to study both valence band and conduction band excitations as well as plasmons. In addition, x-ray Raman scattering involving excitations out of core states can be studied. Because the intrinsic scattering cross section for x rays is ten orders of magnitude smaller than for electrons, the bulk properties of samples can be studied without interference from surface effects as occurs in the case of electron energy loss spectroscopy (EELS). Furthermore, hard x rays do not require the use of ultrahigh-vacuum conditions.

Because scattering rates are significantly reduced for heavily absorbing samples, IXS studies have been limited to materials with low atomic number. Be,[2,3] Li,[4,5] and Al,[6,7] as well as graphite[5] and C$_{60}$,[8] have been studied. A detailed study of Si has also recently appeared.[9] In this work we have extended this list to include the elemental transition metal Ti, as well as the binary material TiC.

The rare combination of strong bonding and metallic conductivity has attracted theoretical attention to the electronic structure of TiC. Furthermore, the simple rocksalt crystal structure has facilitated the calculation of the full dielectric constant $\varepsilon(q,\omega)$ using a full-potential linearized combination of muffin-tin orbitals (LMTO).[10] Here $\hbar\omega$ and $\hbar q$ are the energy and momentum lost by the x-ray photon upon scattering. A sum over the Brillouin zone is required to obtain the wave-vector- and frequency-dependent dielectric constant, and obtaining this sum is an involved procedure.[11]

Broadly speaking, we can divide the IXS processes that involve electronic excitations into two regimes of ω. Plasmons and valence band excitations occur at lower values, and inner shell excitations occur at higher values in the Raman regime. We report here spectral bands for both materials that fall into the plasmon and band excitations regime and are well accounted for by these excitations. In addition, there is for both materials a higher-lying spectral band to which existing theoretical approaches to Raman scattering do not lend an explanation.
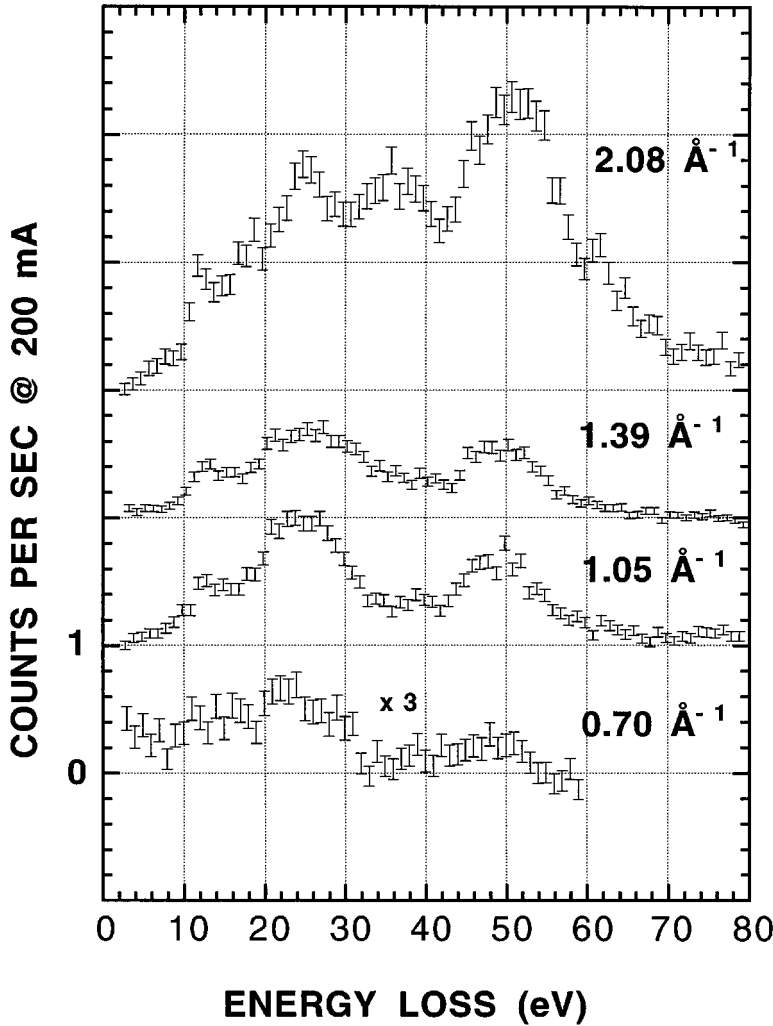
FIG. 1. Spectra obtained for TiC with **q** along [111]. Values for q are shown above the spectra. A value of 1 counts/s is applied to successively offset the spectra.

II. EXPERIMENTAL DETAILS AND RESULTS

The IXS spectra were measured at beam line X21 at the National Synchrotron Light Source. This beam line has a wiggler as a source and delivers 2×10^{11} photons per second in a bandwidth of about 0.7 eV.[12] Crystal analyzers of increased collection efficiency have recently been constructed and were used for the present studies. These analyzers were Si(444) at 7.9 keV (Ref. 12) and Ge(444) at 7.6 keV.[13] Both of these were operated at Bragg angles in the range 86°– 87°. The spectra were obtained by scanning the incident energy with a fixed analyzer setting, i.e., at a fixed collection energy. We used a Ge solid-state detector to record the scattered photons.

We made measurements on single crystals of TiC and Ti. The TiC crystal had a large facet oriented 20° away from [111], and we inclined the crystal by 20° to position the [111] direction along the scattering vector **q**. The Ti crystal was oriented so that **q** lay along $[00\cdot1]$, i.e., along the c axis of the hexagonal structure. The raw spectra for TiC and Ti are shown in Figs. 1 and 2, respectively. The data are shown with low ordinate values of each spectrum brought to the zero of the ordinate scale. The data were normalized to the incident beam by using an ion chamber placed in front of the sample.

III. BASIC RELATIONS AND LOCAL-DENSITY-APPROXIMATION CALCULATIONS

Within the first Born approximation, the double differential cross section is related to the dynamical structure factor $S(\mathbf{q},\omega)$ by the well-known relationship[14]

$$\frac{d^2\sigma}{d\omega\,d\Omega} = (\mathbf{e}_1 \cdot \mathbf{e}_2) r_0^2 \frac{\omega_2}{\omega_1} S(\mathbf{q},\omega), \qquad (1)$$

where $\hbar\omega_1$ and $\hbar\omega_2$ are the energies of the incident and scattered photons, respectively, and $\mathbf{e}_1$ and $\mathbf{e}_2$ are their polarization vectors. The Thomson factor e^2/mc^2 is written as r_0, the classical electron radius. The dynamical structure factor is related to the dielectric response function $\varepsilon(\mathbf{q},\omega)$ by the fluctuation-dissipation theorem[15]

$$S(\mathbf{q},\omega) = -\frac{\hbar q^2}{4\pi^2 e^2 n} \mathrm{Im}\left(\frac{1}{\varepsilon(\mathbf{q},\omega)}\right). \qquad (2)$$

Here n is the electron density.

There are two approaches to the calculation of $1/\varepsilon(\mathbf{q},\omega)$ that have been applied to fitting to $S(\mathbf{q},\omega)$ obtained by IXS.[5] The first approach starts with the jellium model, which reduces the effect of the ion cores to that of a uniform positive background. One proceeds by treating the electron-electron interactions within the random-phase-approximation
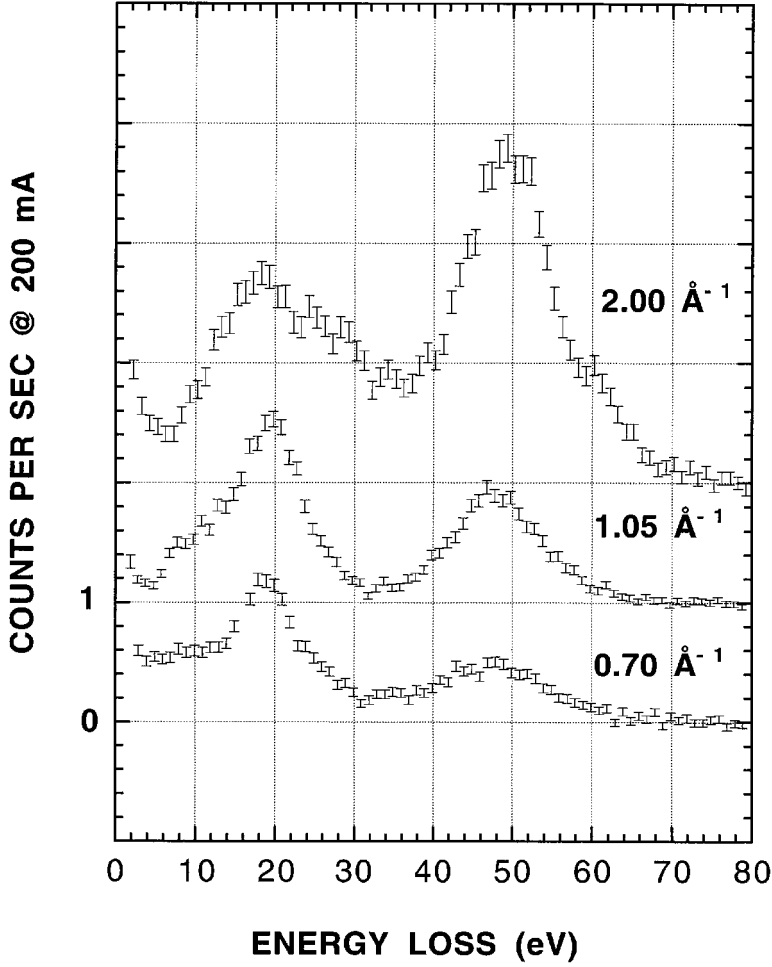
FIG. 2. Spectra obtained for Ti with $\mathbf{q}$ along [00·1]. Values for q are shown, and successive offsets of 1 counts/s were used.

(RPA).[15] In this way the following expression, which is known as Lindhard's longitudinal dielectric function,[16] is obtained:

$$\varepsilon^L(\mathbf{q},\omega)=1-\lim_{\delta\to 0}V_q\sum_{\mathbf{p}}\frac{f(E(\mathbf{p}+\mathbf{q}))-f(E(\mathbf{p}))}{E(\mathbf{p}+\mathbf{q})-E(\mathbf{p})-\hbar\omega+i\delta}.$$

(3)

Here $E(\mathbf{p})$ and $f(E(\mathbf{p}))$ are the single-particle energy and Fermi occupational factor of the eigenstate having a momentum $\mathbf{p}$, and V_q equals $4\pi e^2/q^2\Omega$, with Ω denoting the volume. Corrections for electron-electron interactions beyond the RPA, i.e., for exchange and correlation, are then incorporated via a local field factor[17] and by the introduction of a finite lifetime of the single-particle states.[18] For small q, the Lindhard dielectric constant has a pole corresponding to a plasmon. Within the RPA there is no decay mechanism for the plasmon as long as energy and momentum conservation do not permit the creation of electron-hole pairs. For q larger than q_c, where q_c is defined as the plasmon momentum consistent with the kinematic constraints imposed on electron-hole formation, the plasmon can decay. Plasmon dispersion within the RPA is given by[19]

$$\omega^2=\omega_p^2+\tfrac{3}{5}v_F^2q^2.$$

(4)

Here v_F is the Fermi velocity. Values for n, $\omega_p=\sqrt{4\pi ne^2/m}$, and q_c for TiC and Ti are listed in Table I.

Comparing these to the data, we see that the strong peaks near 24 eV for TiC and near 19 eV for Ti correspond roughly to the expected plasmon energy. Furthermore, of all the q's investigated, the value of 1.05 Å^{-1} is closest to q_c for both TiC and Ti. For values of q larger than q_c, the discrete plasmon excitation couples to the continuum of electron-hole excitations and spectra in this region have been interpreted by including so-called Fano resonances or antiresonances.[9] In addition, the plasmon corresponding to the next reciprocal lattice vector may also be excited.[9] These two phenomena are expected to enter into a complete theoretical description of our data for $q>q_c$.

There are clear peaks in the $S(q,\omega)$ data for TiC taken at $q=1.05$ Å^{-1} at $\sim$12 and $\sim$50 eV that are not explained within the framework of the jellium model as we have outlined it, and the next logical step, the incorporation of band structure, is presented below.

We applied the Ehrenreich-Cohen[20] expression for the dielectric function given by

TABLE I. Free electron values.

	TiC (NaCl)	Ti (hcp)
a, lattice parameter (Å)	4.33	2.95
c, lattice parameter (Å)		4.68
Electrons in unit cell	32	8
n, electron density (Å^{-3})	0.394	0.227
ω_p, plasmon energy (eV)	23.3	17.7
q_c, critical momentum (Å^{-1})	1.09	0.98

$$\varepsilon(q,\omega)=1-\lim_{\delta\to 0}V_q\sum_{r,s,\mathbf{p}}|\langle\Psi_r(\mathbf{p})|e^{-i\mathbf{q}\cdot\mathbf{r}}|\Psi_s(\mathbf{p+q})\rangle|^2\frac{f(E_s(\mathbf{p+q}))-f(E_r(\mathbf{p}))}{E_s(\mathbf{p+q})-E_r(\mathbf{p})-\hbar\omega+i\delta}. \qquad (5)$$

Here r and s are band structure indices. We note that this is the first diagonal element of a more general dielectric matrix with separate elements for separate reciprocal lattice vectors.[19] Neglect of these other terms corresponds to the neglect of microscopic local field effects, i.e., field effects due to the periodicity of the solid.[5] Equation (5) derives from self-consistent field theory[20] and is equivalent to the RPA.[5] Introduction of exchange, correlation, and lifetime effects is thought to be possible via the same techniques as outlined above for the jellium model,[5] although this is a largely untested hypothesis.

However, we have taken a different approach in which we evaluate Eq. (5) using wave functions and eigenvalues derived from local-density-functional theory.[21] This approach incorporates local exchange via the potential of Ceperley and Alder.[22] Due in part to the simple rock salt structure of TiC, we have been able to obtain the dielectric function for $q=1.05$ Å^{-1}. The band sums were performed over the one-electron valence and conduction bands in the first Brillouin zone. Results for Im(ε), Re(ε), and Im($1/\varepsilon$) are shown in Fig. 3. Invoking the fluctuation-dissipation theorem, we compare the calculated values for Im($1/\varepsilon$) to our data in Fig. 4. Here we have convolved the raw calculated results with a Gaussian resolution function having a full width at half maximum (FWHM) of 0.8 eV. This value was measured by

us for the FWHM of the elastic peak of a Plexiglas sample. The ordinate scale was obtained by applying the f-sum rule to both our data and the calculations. The f-sum rule is given by

$$\int \omega S(q,\omega)d\omega=\frac{\hbar q^2}{2m}. \qquad (6)$$

As will be discussed in Sec. IV, we must apply the sum rule to the data without including the peak centered near 50 eV. The integral in Eq. (6) has been performed over the spectrum shown in Fig. 5.

It is convenient at this point to discuss the origin of the peak at 12 eV in Fig. 3. A corresponding peak is clearly evident in the data in Fig. 1. First, we present the l-projected density of states, as shown in Fig. 6. Here we show

$$D_l=\sum_i \delta(E-E_i)w_{l,i}, \qquad (7)$$

where $w_{l,i}$ is the fractional portion of state i with orbital angular momentum quantum number l and lying within the C or Ti muffin-tin spheres. We note that the occupied states (i.e., those below the Fermi energy at about 10 eV on the abscissa scale in Fig. 6) are composed almost entirely of C $2s$ states in a narrow band around 0 eV and of C $2p$–Ti $3d$ bonding states in a strongly hybridized band extending from the Fermi level down about 4 eV. Unoccupied states extending above the Fermi level to about 18 eV are largely antibonding in character. Above 18 eV, the states are mostly free-electron-like, although there are peaks in the density of states at 22 and 25 eV that also have substantial C $2p$ and Ti $3d$ character. One way to separate the contributions to the
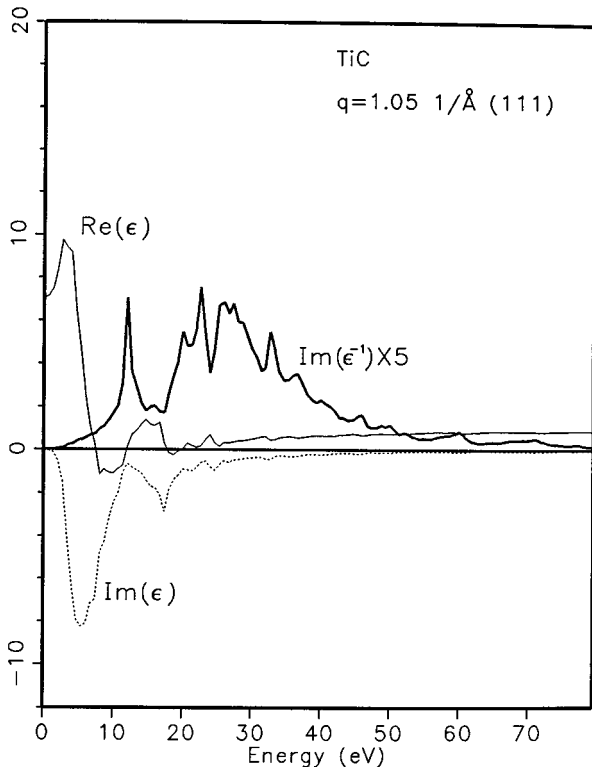
FIG. 3. Calculated values for the real and imaginary parts of the dielectric constant and for Im($1/\varepsilon$) for TiC for $q=1.05$ Å^{-1} along [111].
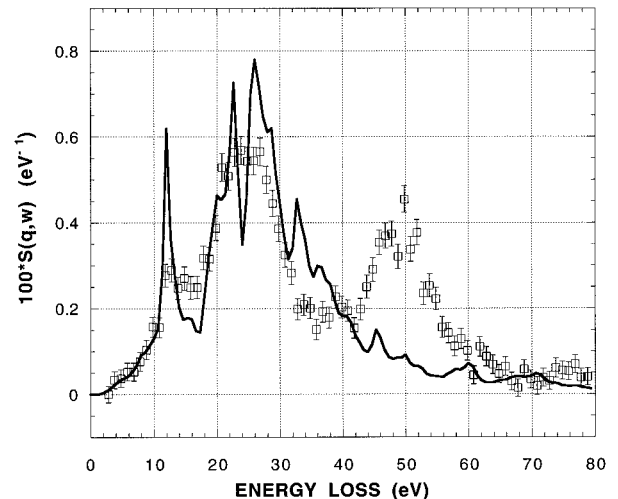
FIG. 4. Data for $S(q,\omega)$ for TiC for $q=1.05$ Å^{-1} (shown as points) compared to results of local-density-functional theory (solid line). Ordinate values were scaled using the f-sum rule.
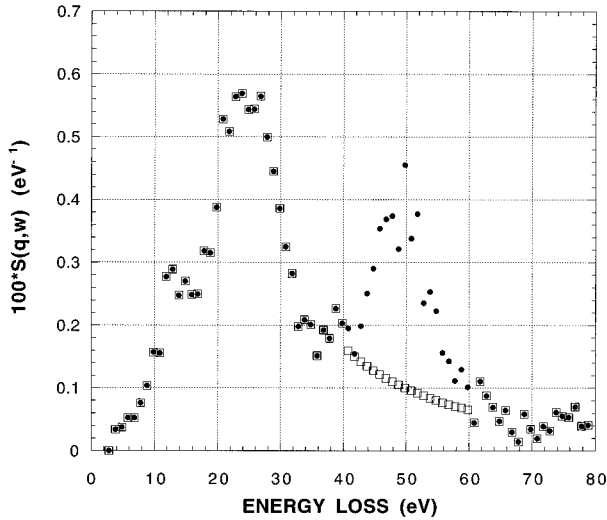
FIG. 5. $S(q,\omega)$ for TiC for $q=1.05$ Å^{-1}. The Raman part of the spectrum was subtracted as shown.

dielectric function of the various bands is to incorporate the weights $w_{l,i}$ into an "l-projected dielectric function." Using a simpler notation with $f_s \equiv (E_s(\mathbf{p}+\mathbf{q}))$ and $f_r \equiv f(E_r(\mathbf{p}))$, we obtain $(f_s - f_r)$ for the factor involving the Fermi functions in Eq. (5). This factor guarantees that the transition is between occupied and unoccupied states. By replacing this factor with

$$(f_s - f_r)(f_s w_{l,s} + f_r w_{l,r}), \tag{8}$$

we obtain an extra factor of $w_{l,s}$ when the s state is occupied and $w_{l,r}$ when the r state is occupied. In either of these cases the transition element is multiplied by the lth partial weight of the occupied state, with no decomposition of the unoccupied state.

In Fig. 7 we show the imaginary part of the dielectric function weighted using Eq. (8). There are two resonances evident at ~ 5 and ~ 18 eV, and these are found to involve transitions out of the C $2p$–Ti $3d$ hybridized band. Results
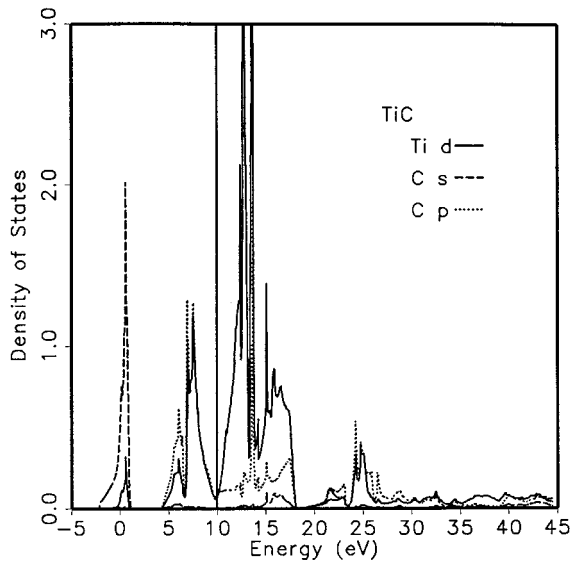
FIG. 6. l-projected density of states for TiC.
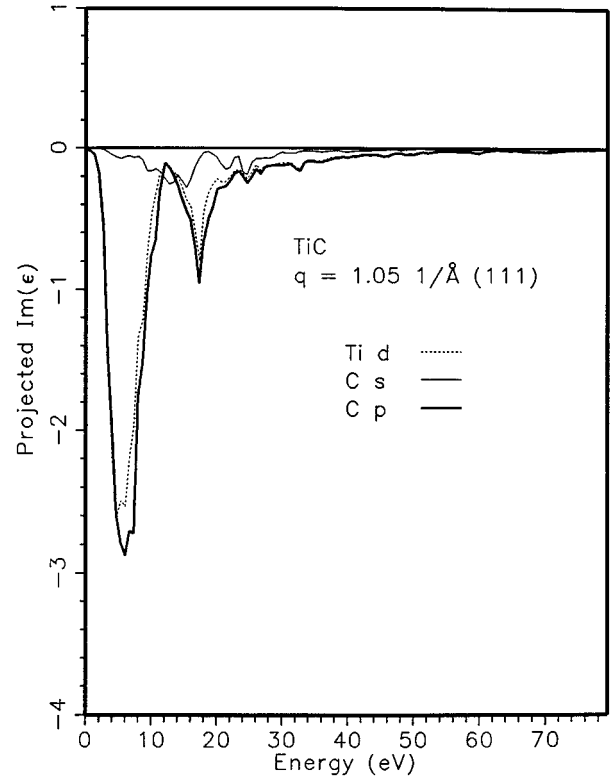
FIG. 7. l-projected values of Im(ε) for TiC for $q=1.05$ Å^{-1} along [111].

for the calculations of the l-projected Re(ε) -1 are shown in Fig. 8. As a rough rule, Re(ε) -1 passes from positive to negative at a resonance.

We are now in a position to comment on the origin of the peak at ~ 12 eV in $S(q,\omega)$. This peak occurs because the minimum between the two resonances in Im(ε) at 5 and 18 eV occurs at about the same point as a zero in Re(ε). The energies of the resonances give a good indication of the unoccupied states involved. We find by means of a more elaborate analysis of the final states that the large resonance at 5 eV arises from transitions to Ti $3d$ and C $2p$ bands in that portion of the density of states centered at ~ 13.5 eV on the abscissa scale in Fig. 6 with most of the transitions going to Ti $3d$. The higher-lying resonance at 18 eV arises from transitions to higher-lying states including a significant contribution of Ti $3d$ and C $2p$ final states lying near ~ 25 eV on the abscissa scale in Fig. 6. There is as well a significant contribution from transitions to other l states in the 18 eV resonance. The higher-lying states are free-electron-like and give rise to excitations that most closely correspond to a plasmon in a free electron picture as discussed above.

IV. RAMAN SCATTERING

From the previous section, it is clear that the peak in all the TiC spectra centered at ~ 50 eV is not encompassed within the previous theoretical framework for valence electron excitations. The fact that the Ti data reveal a similar peak centered at ~ 48 eV strongly suggests that this peak for TiC involves primarily excitations out of the $3p$ band of Ti. We note that a similar peak for both Ti (Ref. 23) and TiC
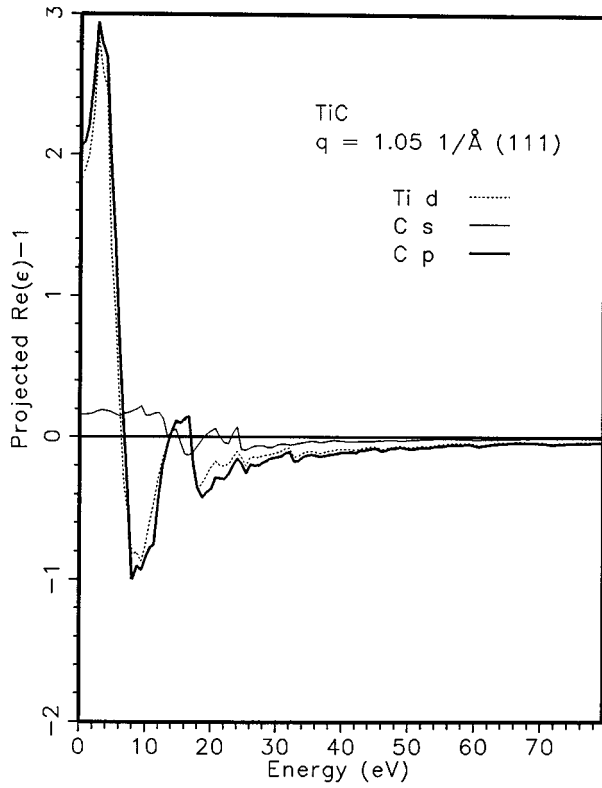
FIG. 8. *l*-projected values of $Re(\varepsilon)-1$ for TiC for $q=1.05$ Å^{-1} along [111].

(Ref. 24) has been observed by EELS. We note that x-ray Raman scattering peaks observed by IXS are referred to as core ionization peaks by the electron scattering community.

X-ray ultraviolet absorption studies and photoelectron spectroscopy studies of $3p$ core excitations for transition-metal atoms reveal rich spectra.[25] In the case of Ti, a multiplet is observed in the absorption spectra. The energies of the multiplet are listed in Table II.

The spectroscopic assignment of the multiplet lines involves $3p^5 3d^{n+1}$ excited states that autoionize into the $3p^6 3d^{n-1} \varepsilon f$ continuum,[26] where εf denotes an electron emitted into a continuum state with predominantly $l=3$ character. Here l is the orbital angular momentum quantum number. Careful absorption studies of Ti films evaporated onto a substrate[27] reveal a single peak centered at 45.9 eV. A pronounced shift towards higher energies for the absorption spectra of Cr metal compared to Cr atoms has also been found.[28] Resonant photoemission has also been applied to the study of $3p$ to $3d$ resonances in transition metals.[29,30] In

TABLE II. Energies for the $3p$ to $3d$ x-ray ultraviolet absorption resonances for atomic Ti.[a]

E (eV)
33.4 ± 0.1
36.6 ± 0.2
38.9 ± 0.1
41.2 ± 0.1
43.5 ± 0.2

[a]Reference 25.

general, an interference between the discrete $3p$ to $3d$ and continuum $3d$ and εl transitions is invoked to explain a shift towards higher energies. A theoretical explanation based on both exchange interaction (between $3d$ electrons and $3p$ holes in the case of transition metals) that splits and raises the multiplet levels and autoionization that broadens the higher levels has been invoked.[31] In support of this picture, we note that autoionized electron emission under 1.5-keV x-ray excitation of Ti has been reported.[32] We note that the autoionization process was invoked to explain similar features in the EELS spectrum of Ti and TiC.[24] Additionally, shake-up excitations, which do not decay into single-hole final states, have also been invoked.[33] Finally, we note that there is a strong peak in the TiC spectrum for $q=2.08$ Å^{-1} centered near 35 eV, a value between the lowest two absorption resonances listed in Table II. We surmise that this peak corresponds to the actual onset of the $3p$ to $3d$ absorption edge, but this conclusion must await further theoretical developments.

A theory of x-ray Raman scattering has been formulated based on a one-electron picture and has yielded the Golden rule relationship[34–36]

$$S_R(\mathbf{q},\omega) = \sum_{\mathbf{p}} |\langle \mathbf{p}| e^{i\mathbf{q}\cdot\mathbf{r}}|0\rangle|^2 \delta(E(\mathbf{p})-E(0)-\hbar\omega). \quad (9)$$

When analyzed within the dipole approximation and when applied to an isotropic solid, one obtains

$$S_R(\mathbf{q},\omega) = \frac{cq^2}{4\pi^2 e\omega}\sigma(\omega), \quad (10)$$

where $\sigma(\omega)$ is the soft x-ray absorption cross section. If Eq. (10) applies, the Raman spectrum should have essentially the same shape as the absorption spectrum.[36]

Our data do not reveal a clear absorption edge followed by a plateau as was observed for x-ray Raman spectra of Li.[5] This qualitative difference for our data casts suspicion on the approximations made in deriving Eq. (10). An analysis of the q dependence of our Ti data confirms the inadequacy of Eq. (10) in describing our Raman results. We applied the f-sum rule, which is derived from a particle conservation condition,[15] to place the ordinate on an absolute scale for $S(q,\omega)$ of the valence electron excitations. Following Nagasawa, Mourikis, and Schulke,[36] the sum rule was applied after subtracting the Raman portion of the spectrum as shown in Fig. 9. The peak amplitude above the tail of the valence electron excitations is plotted as a function of q^2 in the upper panel of Fig. 10. We find that the q^2 dependence of Eq. (10) does not hold. We find instead a logarithmic dependence as shown in the lower panel of Fig. 10. Only terms that are higher order in q (e.g., quadrupole) are expected based on Eq. (9), and consequently we conclude that the above theoretical description does not apply to our experimental results.

V. SUMMARY AND CONCLUSIONS

Inelastic x-ray scattering spectra for TiC and Ti are reported. The spectra are informative not only about valence excitations, but also about high-energy loss excitations out of the $3p$ core states of Ti. The valence excitations are com-
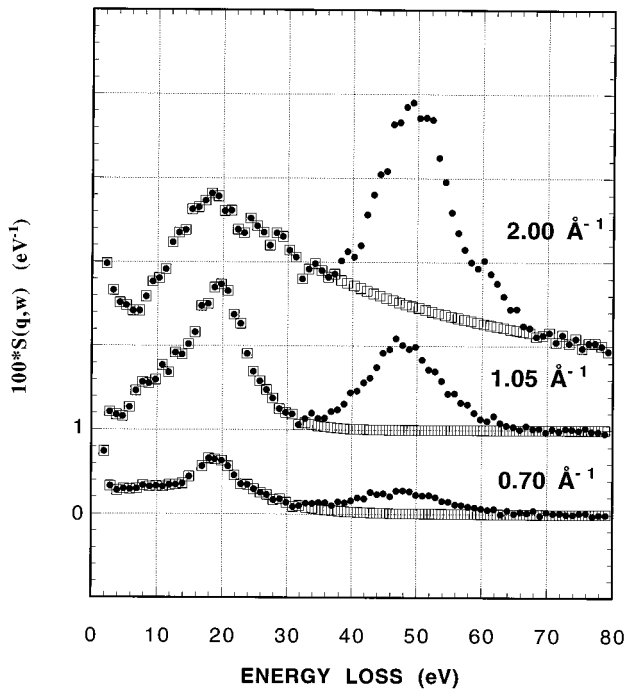
FIG. 9. $S(q,\omega)$ for Ti. The ordinate scale was obtained from the IXS data by applying the f-sum rule to the points shown as squares. The Raman contribution to the spectrum is the difference between the data shown as solid circles and squares.

FIG. 10. Peak Raman contribution to $S(q,\omega)$ plotted vs q^2 in the top part of the figure and vs $\log(q)$ in the bottom part.

pared to results of calculations made using local-density-functional theory, and we find that we can relate certain spectral features to band transitions. The q dependence of the core excitation part of the spectrum disagrees with a one-electron theoretical description applied to an isotropic solid.

[1] W. Schulke, in *Handbook on Synchrotron Radiation*, edited by G. Brown and D. Moncton (North-Holland, Amsterdam, 1991), Vol. 3, pp. 565–637.

[2] P. Eisenberger, P. M. Platzman, and K. C. Pandy, Phys. Rev. Lett. **31**, 311 (1973).

[3] W. Schulke, H. Nagasawa, S. Mourikis, and A. Kaprolat, Phys. Rev. B **40**, 12 215 (1989).

[4] P. Eisenberger, P. M. Platzman, and P. Schmidt, Phys. Rev. Lett. **34**, 18 (1975).

[5] W. Schulke, H. Nagasawa, S. Mourikis, and P. Lanzki, Phys. Rev. B **33**, 6744 (1986).

[6] P. M. Platzman and P. Eisenberger, Phys. Rev. Lett. **33**, 152 (1974).

[7] P. M. Platzman, E. D. Isaacs, H. Williams, P. Zschack, and G. Ice, Phys. Rev. B **46**, 12 943 (1992).

[8] E. D. Isaacs, P. M. Platzman, P. Zschack, K. Hamalainen, and A. R. Kortan, Phys. Rev. B **46**, 12 910 (1992).

[9] W. Schulke, J. R. Schmitz, H. Schulte-Schrepping, and A. Kaprolet, Phys. Rev. B **52**, 11 721 (1995).

[10] D. L. Price and B. R. Cooper, Phys. Rev. B **39**, 4945 (1989).

[11] J. P. Walter and M. L. Cohen, Phys. Rev. B **5**, 3101 (1972).

[12] C. C. Kao, K. Hamalainen, M. Krisch, D. P. Siddons, T. Oversluizen, and J. B. Hastings, Rev. Sci. Instrum. **66**, 1699 (1995).

[13] A. T. Macrander, V. I. Kushnir, and R. C. Blasdell, Rev. Sci. Instrum. **66**, 1546 (1995).

[14] P. Nozieres and D. Pines, Phys. Rev. **113**, 1254 (1959).

[15] D. Pines and P. Nozieres, *The Theory of Quantum Liquids* (Benjamin, New York, 1996), Vol. 1.

[16] J. Lindhard, Kgl, Danske Videnskab. Selskab Mat. Fys. Medd. **28**, 8 (1954).

[17] J. Hubbard, Proc. R. Soc. London A **243**, 336 (1957).

[18] G. Mukhopadhyay, R. K. Kalia, and K. S. Singwi, Phys. Rev. Lett. **34**, 950 (1975).

[19] P. M. Platzman and P. A. Wolff, *Waves and Interactions in Solid State Plasmas* (Academic, New York, 1973).

[20] H. E. Ehrenreich and M. H. Cohen, Phys. Rev. **115**, 786 (1959).

[21] *Theory of the Inhomogeneous Electron Gas*, edited by S. Lundquist and N. H. March (Plenum, New York, 1983).

[22] D. M. Ceperley and B. J. Alder, Phys. Rev. Lett. **45**, 566 (1980).

[23] C. Wehenkel and B. Gauthe, Phys. Status Solidi B **64**, 515 (1974).

[24] Y. Chan, D. Liao, S. W. Lee, B. R. Cooper, and P. A. Montano, Z. Phys. B **87**, 117 (1992).

[25] B. Sonntag and P. Zimmermann, Rep. Prog. Phys. **55**, 911 (1992).

[26] M. Meyer, Th. Prescher, E. von Raven, M. Richter, E. Schmidt, B. Sonntag, and H. E. Wetzel, Z. Phys. D **2**, 347 (1986).

[27] B. Sonntag, R. Haensel, and C. Kunz, Solid State Commun. **7**, 597 (1969).

[28] J. T. Costello, E. T. Kennedy, B. F. Sonntag, and C. W. Clark, Phys. Rev. A **43**, 1441 (1991).

[29] G. Zajac, S. D. Bader, A. J. Arko, and J. Zak, Phys. Rev. B **29**, 5491 (1984).

[30] S. D. Bader, G. Zajac, A. J. Arko, M. B. Brodsky, T. I. Morrison, J. Zak, R. L. Benbow, and Z. Hurych, Phys. Rev. B **33**, 3636 (1986).

[31] J. L. Dehmer, A. F. Starace, U. Fano, J. Sugar, and J. W. Cooper, Phys. Rev. Lett. **26**, 1521 (1971).

[32] R. Brenner, J. Felsteiner, R. Tyk, and J. Zak, Phys. Rev. B **37**, 1387 (1988).

[33] J. Barth, F. Gerken, and C. Kunz, Phys. Rev. B **31**, 2022 (1985).

[34] Y. Mizuno and Y. Ohmura, J. Phys. Soc. Jpn. **22**, 445 (1967).

[35] S. Doniach, P. M. Platzman, and J. T. Yue, Phys. Rev. B **4**, 3345 (1971).

[36] H. Nagasawa, S. Mourikis, and W. Schulke, J. Phys. Soc. Jpn. **58**, 710 (1989).